Power Test of the First Two HL-LHC Insertion Quadrupole Magnets Built at CERN

F. J. Mangiarotti, G. Willering, L. Fiscarelli, M. Bajko, L. Bottura, V. Desbiolles, A. Devred, *Senior Member, IEEE*, J. Ferradas Troitino, S. Izquierdo Bermudez, R. Keijzer, F. Lackner, A. Milanese, G. Ninet, H. Prin, E. Ravaioli, S. Russenschuck, E. Takala, and E. Todesco

***Abstract*—The High-Luminosity project (HL-LHC) of the CERN Large Hadron Collider (LHC), requires low β* quadrupole magnets in Nb $_3$Sn technology that will be installed on each side of the ATLAS and CMS experiments. After a successful short-model magnet manufacture and test campaign, the project has advanced with the production, assembly, and test of full-size 7.15-m-long magnets. In the last two years, two CERN-built prototypes (MQXFBP1 and MQXFBP2) have been tested and magnetically measured at the CERN SM18 test facility. These are the longest accelerator magnets based on Nb $_3$Sn technology built and tested to date. In this paper, we present the test and analysis results of these two magnets, with emphasis on quenches and training, voltage-current measurements and the quench localization with voltage taps and a new quench antenna.**

***Index Terms*—Low beta quadrupole, Nb_3Sn, quench, superconducting magnets.**

I. Introduction

AS PART of the HL-LHC project at CERN, the Nb-Ti inner triplet quadrupole magnets near the ATLAS and CMS interaction points will be replaced with large aperture Nb $_3$Sn quadrupole magnets, named MQXF [1], [2]. These magnets are developed, manufactured, and tested in a collaboration between CERN and the US HL-LHC Accelerator Upgrade Project (AUP). The MQXF program includes the construction and test of several short-length model magnets, the 4.2-m-long magnets for Q1 and Q3 (constructed by AUP [3]), and the 7.15-m-long magnets for Q2a and Q2b (MQXFB, constructed by CERN). The first two MQXFB full-length prototype magnets (MQXFBP1 and MQXFBP2) were manufactured, assembled and cryostated at CERN [4]. MQXFBP1 was tested in summer–fall 2020, and MQXFBP2 was tested in winter–spring and fall 2021. Key figures of these two prototype magnets are shown in Table I, and the coils used in each magnet in Table II.

TABLE I
MQXFBP1 and MQXFBP2 Main Parameters

Parameter	MQXFBP1	MQXFBP2
Aperture	150 mm	
Nominal operation energy level	7 TeV	
Nominal gradient	133 T/m	
Nominal current	16.23 kA	
Nominal peak field	11.4 T	
Nominal stored energy	8.37 MJ	
Magnetic length	7.15 m	
Short sample limit (1.9 K)	22.2 kA	22.0 kA
Short sample limit (4.5 K)	19.9 kA	19.8 kA

TABLE II
Coils Used in MQXFBP1 and MQXFBP2

Magnet	P1	P2	P3	P4
MQXFBP1	CR105	CR104	CR108	CR107
MQXFBP2	CR113	CR112	CR111	CR110

II. Test Plan and Features

A. Magnet Powering, Quench Detection and Protection

MQXFBP1 and MQXFBP2 were tested in the A1 horizontal test bench at the SM18 magnet test facility at CERN [5]. The magnets were powered with a 1-quadrant, 20 kA DC power converter. In addition, during the MQXFBP2 test campaign, an additional 1-quadrant, 2 kA DC power converter was used for *trimmed powering* tests: the current in one of the coils was reduced for diagnostic purposes. The circuit diagram is shown in Fig. 1.

The magnets were tested using the baseline quench detection and protection systems for operation in the LHC:

- Quench detection with a universal quench detection system (uQDS, see [6]), which allows to set variable voltage thresholds and validation windows depending on the magnet current.
- Magnet protection with outer-layer quench heaters [7], [8] and coupling-loss induced quench system (CLIQ [9]). Energy extraction by means of a dump resistor was not used for these magnets.

Manuscript received November 26, 2021; revised February 13, 2022 and February 21, 2022; accepted February 28, 2022. Date of publication March 8, 2022; date of current version March 25, 2022. *(Corresponding author: F. J. Mangiarotti.)*

F. J. Mangiarotti, G. Willering, L. Fiscarelli, M. Bajko, L. Bottura, V. Desbiolles, A. Devred, J. Ferradas Troitino, S. Izquierdo Bermudez, F. Lackner, A. Milanese, G. Ninet, H. Prin, E. Ravaioli, S. Russenschuck, E. Takala, and E. Todesco are with CERN, CH-1211 Geneva, Switzerland (e-mail: franco.julio.mangiarotti@cern.ch).

R. Keijzer is with CERN, CH-1211 Geneva, Switzerland, and also with Universiteit Twente, 7522 Enschede, The Netherlands (e-mail: ruben.keijzer@cern.ch).

Color versions of one or more figures in this article are available at https://doi.org/10.1109/TASC.2022.3157574.

Digital Object Identifier 10.1109/TASC.2022.3157574

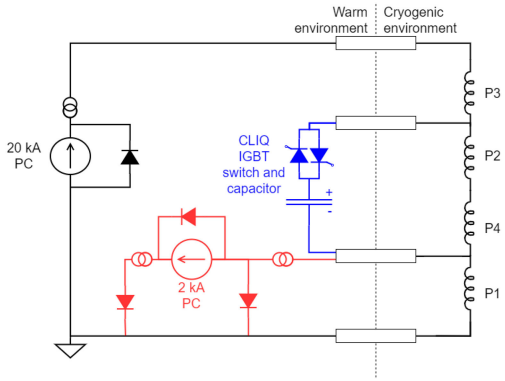

Fig. 1. Circuit diagram for the test of MQXFB prototypes. PC indicates the DC power converters. Black shows the standard powering circuit. Blue corresponds to the CLIQ system. Red shows the additional powering circuit for the trimmed powering of pole P1. The blue and red circuits were not connected simultaneously.

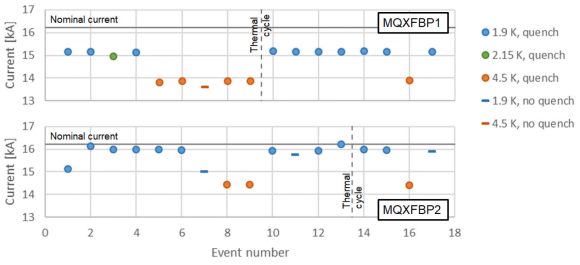

Fig. 2. Natural quench history at nominal test ramp rate of MQXFBP1 (top) and MQXFBP2 (bottom).

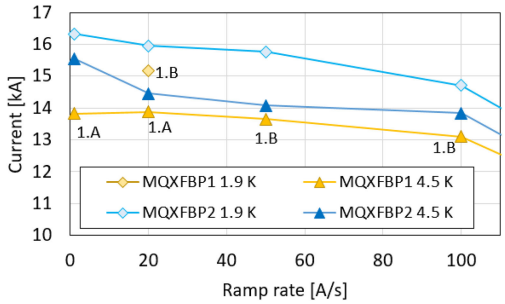

Fig. 3. Quench current vs. ramp rate at 1.9 and 4.5 K of MQXFBP1 and MQXFBP2. Quenches in MQXFBP2 were all quench location 2.A; the location of quenches in MQXFBP1 is noted next to each point.

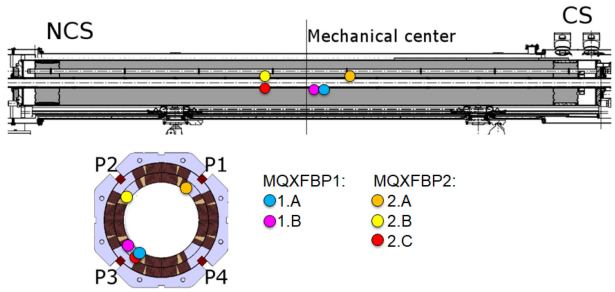

Fig. 4. Longitudinal location (top) and in the cross section (bottom left) of the recurring quenches in the MQXFB prototypes, based on the voltage taps and quench antenna measurements.

B. Magnet Instrumentation

The four coils of both prototypes were instrumented with 8 voltage taps in each of their two layers, for a total of 64 voltage taps per magnet. Of these, only 8 (plus redundancy) are required for LHC operation, one voltage tap at each extremity of each coil. The remaining 56 voltage taps were installed to be used for quench localization and performance analysis.

In addition, the magnets were instrumented with strain gauges on the rods and with optical fibers with Bragg gratting (FBG) sensors in the coil poles [10]; MQXFBP1 was also equipped with strain gauges on the magnet shell. The mechanical measurements will be reported in another publication.

On the test bench, the magnets were equipped with an *anti-cryostat*, that allows the bore to be accessible at room temperature during magnet operation. This allowed us to use a dedicated array of induction coils that can be used for quench localization, usually referred to as *quench antenna*, and a stretched wire or a rotating-coil magnetometer for magnetic field measurements.

III. Test and Measurement Results

A. Quench Performance

The natural quench history at nominal test ramp rate (20 A/s) of the two magnets is shown in Fig. 2. Training was done at 1.9 K. MQXFBP1 reached a quench limit during the first ramp to quench, at 15.17 kA (93.4% of the nominal current). MQXFBP2 reached its limit at the second ramp to quench, at 15.95 kA (98.2% of nominal current). In each magnet, the quenches at the quench limit had the same signature, in terms of resistive voltage growth rate, coil segment that quenched, and quench antenna signals.

Further investigation of the quench performance was done at different temperature levels (1.9, 2.15 and 4.5 K) and ramp rates (1, 20, 50, 100, 150 and 200 A/s). The quenches at 100 A/s and below were in the inner-layer pole turn straight section, close to the magnet mechanical center. In MQXFBP1, these quenches were in pole P3, on the left of the pole at low ramp rate (location 1.A) and on the right of the pole at higher ramp rate (1.B). In MQXFBP2, the quenches were on pole P1, always on the left of the pole (location 2.A). Quenches above 100 A/s were in the inner-layer multi-turn blocks, near the magnet heads, and are attributed to heating due to high AC losses. A summary of the quench current at 100 A/s and below is shown in Fig. 3. The quench locations are shown in Fig. 4.

The resistive voltage development after quench was compared to previous experience in MQXF short-model magnets. For both magnets, the resistive voltage growth was similar or slower than in the short models at similar current, see an example for MQXFBP2 in Fig. 5. The quench propagation velocity at 1.9 K in both magnets is around 60–70 m/s.

Longitudinal quench localization was done by shifting the quench antenna along the magnet axis: coarse localization was done with nine 600-mm-sectors that cover most of the magnet.

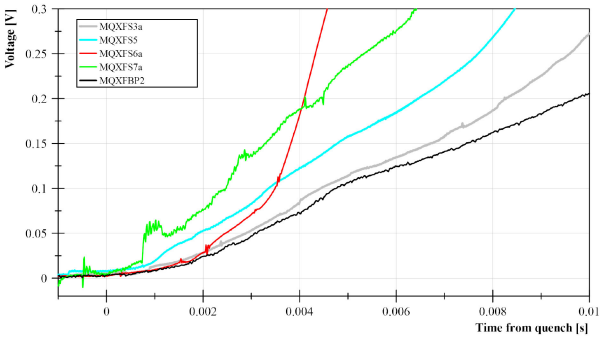

Fig. 5. Resistive voltage development in the recurring quench location at 20 A/s, 1.9 K in MQXFBP2 (black) compared to quenches in the short models at similar current. In all cases the quench location is similar (inner-layer pole turn or adjacent turns).

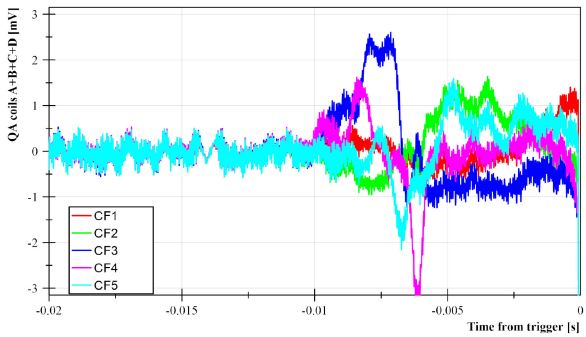

Fig. 6. Example of quench antenna signals after a quench in MQXFBP2. Signals CF1 through CF4 correspond to the 50 mm coils; CF5 corresponds to the 100 mm coil. In this case, quench antenna segments CF3 and CF4 react to the quench first, around time −10 ms, indicating that the quench starts in that location.

Once a recurring quench location was identified, the localization was narrowed-down by shifting the quench antenna 200–300 mm along the axis. A last step of localization was done by placing the quench antenna end (consisting of four 50 mm, one 100 mm and one 300 mm induction coils) around the quench location. This last step allows to identify the quench location within ±50 mm. One example of quench antenna signal for the last localization step is shown in Fig. 6.

B. Magnetic Measurements

Magnetic field measurements were performed in both magnets at low current and room temperature with rotating-coil magnetometers, and at the highest stable current at 1.9 K with the stretched wire. In addition, for MQXFBP2 the magnetic field was measured with rotating-coil magnetometers at 1.9 K. The transfer function measured on MQXFBP2 is +60 units in 10000 with respect to MQXFBP1. This difference is not visible on measurements at ambient temperature. About +20 units can be explained by the presence of magnetic shims. A summary of transfer function measurements at 1.9 K is given in Fig. 7.

The field quality in both magnets is within specifications. A systematic b6 component of about −5 units is present on MQXFBP1. It has been later corrected by removing 0.125 mm from the midplane before impregnation. The effectiveness of the correction is visible on MQXFBP2. In addition, based on

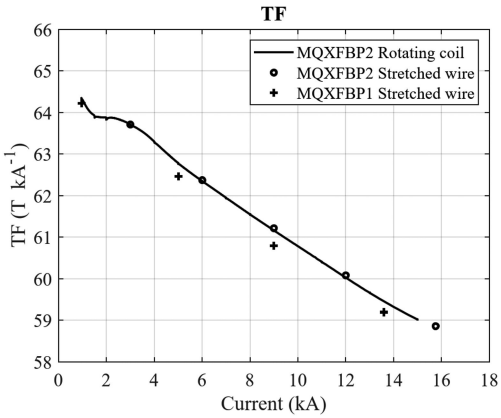

Fig. 7. Transfer function measurements in MQXFBP1 and MQXFBP2, performed during a stairstep current cycle. The transfer function measured on MQXFBP2 is +60 unit compared to MQXFBP1.

TABLE III
FIELD QUALITY IN MQXFBP1 AND MQXFBP2, IN TERMS OF INTEGRAL FIELD, AT 50 MM REFERENCE RADIUS. VALUES IN UNITS OF 10^{-4}. MAGNETIC SHIMS WERE INSTALLED IN MQXFBP2 TO CORRECT THE B3 COMPONENT FOLLOWING THE MEASUREMENTS AT 300 K

	MQXFBP1		MQXFBP2			
	300 K		300 K		1.9 K, 15 kA	
n	bn	an	bn	an	bn	an
3	0.02	-0.19	3.94	-0.75	1.11	-1.71
4	0.38	-0.59	0.59	1.50	0.93	1.25
5	-0.46	-0.18	0.08	1.04	-0.2	1.43
6	-4.99	-0.1	-0.89	0.07	0.32	-0.04
7	-0.1	0.02	0.24	-0.17	0.26	-0.27
8	0.03	-0.12	0.17	0.04	0.02	0.06
9	-0.08	-0.01	-0.11	-0.08	0.23	-0.11
10	-0.35	-0.01	-0.25	0.06	-0.34	0.03

the room temperature measurements, magnetic shims were installed in MQXFBP2 to correct b3. The correction resulted to be effective at nominal level (b3 $<$ 2 units). A summary of the magnetic field quality at both temperatures in Table III

C. V-I Measurements

V-I measurements (see [3], [12]) have been done in both MQXFB prototype magnets. During uniform stair-step current cycles in MQXFBP1 decaying voltages were observed in the quenching locations and the segment between them (corresponding to the inner layer pole turn head) upon reaching a current plateau near the quench current. The voltage decay is negative in quench location 1.A, and positive in the other two segments. At that current level, the voltage decays to a level above the previous current plateau, indicating the start of the superconducting normal transition. This is shown in Fig. 8.

In MQXFBP2, during a similar uniform stair-step curreny cycle, the decaying voltage in the quench location is much smaller, and mainly a non-decaying voltage increase is observed. Further investigations were done with a current cycle with a higher density current step near the quench current, and the start of the superconducting-normal transition could be better measured. In Fig. 9 the results in the quench location segment for

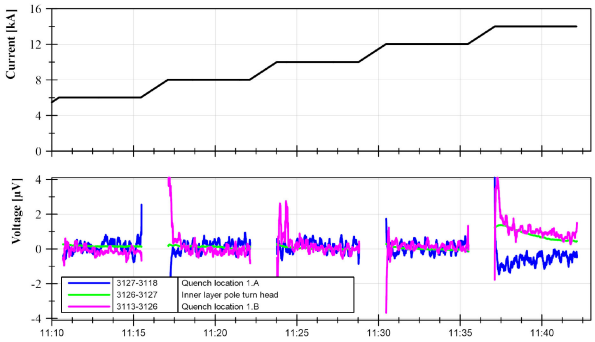

Fig. 8. V-I measurements in MQXFBP1, shown as current and voltage versus time, during an uniform stair-step current cycle. During the last current plateau a voltage offset and decay can be observed.

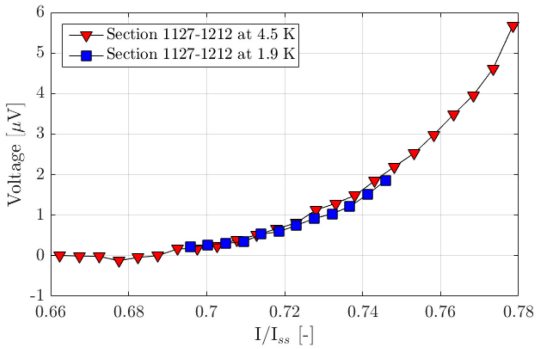

Fig. 9. V-I measurements the quench location segment in MQXFBP2, at 1.9 (blue) and 4.5 K (red), during a current cycle with high density of current plateaus near the quench current. The current has been normalized to the short sample limit at each temperature. Note that the magnetic field in the measured segment increases with the current. The quench happens at a lower fraction of short sample limit at 1.9 K. Error bars in the vertical axis are around 0.1 μV (not shown).

such tests is shown, at 1.9 and 4.5 K, with the current normalized to the short sample limit indicated in Table I. The inner pole turn segments of the other coils also show an early start of the transition, at up to 1/5 of the voltage level of the quench-location segment.

D. Trimmed Powering of MQXFBP2

In preparation for the trimmed powering of MQXFBP2, the powering setup, quench behavior and agreement with simulations were tested on the short magnet MQXFS7b [13], [14], and the protection scheme without CLIQ was verified at increasing currents in MQXFBP2. The magnet was then ramped to quench at 1.9 and 4.5 K, using a trim current of 0, 2.5 and 5% of the main current. The results of trimmed powering is shown in Fig. 10. With a 5% trim, pole P3 quenches in location 2.C at 20 A/s (1.9 and 4.5 K), pole P2 quenches in location 2.B at 1 A/s, 4.5 K, and no quench is recorded up to 17 kA at 1 A/s, 1.9 K. All quenches were in the inner layer pole turn straight segment of the respective coils.

IV. Discussion

Both magnets have similar behavior: they have a quench current limit in the inner pole turn of one coil, near the mechanical

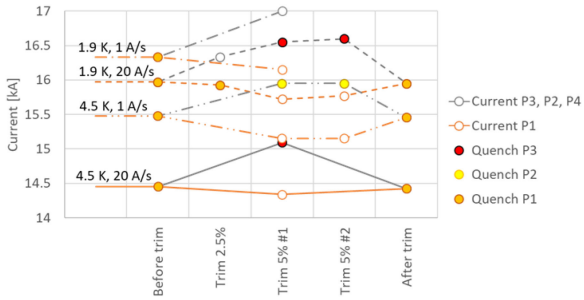

Fig. 10. Trimmed powering quench summary of MQXFBP2. Quenches in P2 are in quench location 2.B, and in P3 in quench location 2.C.

center. Their ramp rate and temperature dependency is mostly "normal". Both magnets show early superconducting-normal transition observed in the quench location segments, with decaying voltages. The quench propagation velocity is similar to other MQXF short magnets at similar quench current. All these indicators point towards local damage of the superconductor, as opposed to distributed (over several twist pitches) degradation as was seen in early short models of the CERN 11 T Nb_3Sn dipole [15], [16].

The decaying voltages in the MQXFBP1 V-I measurements during current flat-tops indicate current redistribution between strands, likely caused by a non-uniform degradation component. Also, negative decaying voltages cannot be explained by damage in the segment measured. This topic is discussed in detail in [12]. For such type of degradation, the expected degradation location would be the quench location at high ramp rate and high temperature, in this case location 1.B. In MQXFBP2, the expected degradation location is the quench location.

V. Conclusion

The first two MQXFB prototypes magnets have been power tested at the CERN SM18 test facility. MQXFBP1 reached 15.17 kA (93.4% of nominal current, corresponding to an operation energy of 6.5 TeV) and MQXFBP2 reached 15.95 kA (98.2% of nominal current, corresponding to 6.9 TeV).

The field quality of the two tested magnets resulted to be within specifications. A systematic b6, present on MQXFBP1 and already seen on the short models, has been successfully corrected by shimming the coil midplane. On MQXFBP2, the b3 component has been corrected by applying magnetic shims in the bladder slots.

The performance limitation in both MQXFB prototypes is expected to be caused by local damage of the superconductor, in the quench location at high ramp rate. This location was identified within $\pm$50 mm, to allow further investigation at room temperature.

Trimmed powering of the limiting coil in MQXFBP2 allowed the other three coils to be powered above the performance limit. With a 5% trim, other two coils quenched at around 500–600 A higher than the limiting coil at the same temperature and ramp rate conditions.

REFERENCES

[1] E. Todesco *et al.*, "A first baseline for the magnets in the high luminosity LHC insertion regions," *IEEE Trans. Appl. Supercond.*, vol. 24, no. 3, Jun. 2014, Art. no. 4003305.

[2] E. Todesco *et al.*, "The high luminosity LHC interaction region magnets towards series production," *Supercond. Sci. Technol.*, vol. 34, 2021, Art. no. 053001.

[3] G. Ambrosio *et al.*, "Lessons Learned From the Prototypes of the MQXFA Low-Beta Quadrupoles for HL-LHC and Status of Production in the US," *IEEE Trans. Appl. Supercond.*, vol. 31, no. 5, Aug. 2021, Art. no. 4001105.

[4] S. I. Bermudez *et al.*, "Progress in the development of the Nb_3Sn MQXFB quadrupole for the HiLumi upgrade of the LHC," *IEEE Trans. Appl. Supercond.*, vol. 31, no. 5, Aug. 2021, Art. no. 4002007.

[5] M. Bajko, "SM18 the CERN magnet test facility," Accessed: Feb. 11, 2022. [Online]. Available: https://indico.cern.ch/event/704235/contributions/2931988/

[6] R. Denz *et al.*, "Quench detection and diagnostic systems for the superconducting circuits for the HL-LHC," in *Proc. 10th Int. Part. Accel. Conf.*, Melbourne, Australia, May 2019, Art. no. THPTS036.

[7] S. I. Bermudez *et al.*, "Overview of the quench heater performance for MQXF, the Nb_3Sn Low-β quadrupole for the high luminosity LHC," *IEEE Trans. Appl. Supercond.*, vol. 28, no. 4, Jun. 2018, Art. no. 4008406.

[8] E. Ravaioli *et al.*, "Quench protection performance measurements in the first MQXF magnet models," *IEEE Trans. Appl. Supercond.*, vol. 28, no. 3, Apr. 2018, Art. no. 4701606.

[9] E. Ravaioli, "CLIQ," Ph.D. dissertation, Univ. Twente, 2015.

[10] L. Bianchi, "Strain measurements on MQXFBP1 superconducting magnet," CERN, Tech. Rep. EDMS 1851752, 2021.

[11] F. J. Mangiarotti *et al.*, "Powering Performance and Endurance Beyond Design Limits of HL-LHC Low-Beta Quadrupole Model Magnets," *IEEE Trans. Appl. Supercond.*, vol. 31, no. 5, Aug. 2021, Art. no. 4000805.

[12] R. Keijzer *et al.*, "Modelling V-I measurements of Nb_3Sn accelerator magnets with conductor degradation," *IEEE Trans. Appl. Supercond.*, to be published, doi: 10.1109/TASC.2022.3153247.

[13] F. Mangiarotti, "MQXFS7b trim test results," CERN, Tech. Rep. EDMS 2621655, 2021.

[14] E. Ravaioli, "Analysis of the electrical and thermal behavior of coil 211 of the MQXFS7b magnet," CERN, Tech. Rep. EDMS 2645040, 2021.

[15] G. Willering *et al.*, "Comparison of cold powering performance of 2-m-Long Nb_3Sn 11 T. model magnets," *IEEE Trans. Appl. Supercond.*, vol. 28, no. 3, Apr. 2018, Art. no. 4007205 .

[16] F. J. Mangiarotti *et al.*, "Quench propagation in Nb_3Sn cos-theta 11 T. dipole model magnets in high stress areas," *IEEE Trans. Appl. Supercond.*, vol. 28, no. 4, Jun. 2018, Art. no. 4008204.